ICARUS 58, 137–152 (1984)

The Chaotic Rotation of Hyperion*

JACK WISDOM AND STANTON J. PEALE

Department of Physics, University of California, Santa Barbara, California 93106

AND

FRANÇOIS MIGNARD

Centre d'Etudes et de Recherches Géodynamique et Astronomique, Avenue Copernic, 06130 Grasse, France

Received August 22, 1983; revised November 4, 1983

A plot of spin rate versus orientation when Hyperion is at the pericenter of its orbit (surface of section) reveals a large chaotic zone surrounding the synchronous spin–orbit state of Hyperion, if the satellite is assumed to be rotating about a principal axis which is normal to its orbit plane. This means that Hyperion's rotation in this zone exhibits large, essentially random variations on a short time scale. The chaotic zone is so large that it surrounds the 1/2 and 2 states, and libration in the 3/2 state is not possible. Stability analysis shows that for libration in the synchronous and 1/2 states, the orientation of the spin axis normal to the orbit plane is unstable, whereas rotation in the 2 state is attitude stable. Rotation in the chaotic zone is also attitude unstable. A small deviation of the principal axis from the orbit normal leads to motion through all angles in both the chaotic zone and the attitude unstable libration regions. Measures of the exponential rate of separation of nearby trajectories in phase space (Lyapunov characteristic exponents) for these three-dimensional motions indicate the the tumbling is chaotic and not just a regular motion through large angles. As tidal dissipation drives Hyperion's spin toward a nearly synchronous value, Hyperion necessarily enters the large chaotic zone. At this point Hyperion becomes attitude unstable and begins to tumble. Capture from the chaotic state into the synchronous or 1/2 state is impossible since they are also attitude unstable. The 3/2 state does not exist. Capture into the stable 2 state is possible, but improbable. It is expected that Hyperion will be found tumbling chaotically.

I. INTRODUCTION

The rotation histories of the natural satellites have been summarized by Peale (1977). Most of the natural satellites fall into one of the two well-defined categories: those which have evolved significantly due to tidal interactions and those which have essentially retained their primordial spins. The exceptions are Hyperion and Iapetus, for which the time scales to despin to spin rates which are synchronous with their respective orbital mean motions are estimated to be on the order of one billion years. However, it has been known for some time that Iapetus rotates synchronously (Widorn, 1950). Since the time scale for the despinning of Hyperion is somewhat less than that for Iapetus, it is likely that Hyperion has significantly evolved as well.

As a satellite tidally despins, it may be captured in a variety of spin–orbit states where the spin rate is commensurate with the orbital mean motion. Mercury, however, is the only body in the solar system which is known to have a nonsynchronous yet commensurate spin rate (see Goldreich and Peale, 1966). Among the tidally evolved natural satellites, where the spin rates are known the satellites are all in synchronous rotation, and in those cases where the spin rate is not known the probability of capture in a nonsynchronous state

* Paper presented at the "Natural Satellites Conference," Ithaca, N.Y., July 5–9, 1983.

0019-1035/84 $3.00

is small. Most of the tidally evolved satellites are expected to be synchronously rotating. Hyperion is the only remaining possibility for an exotic spin–orbit state (see, e.g., Peale, 1978). We shall see that it may indeed be exotic.

In their original paper on spin–orbit coupling, Goldreich and Peale (1966) derive a pendulum-like equation for each spin–orbit state by rewriting the equations of motion in terms of an appropriate resonance variable and eliminating the nonresonant, high-frequency contributions through averaging. The strength of each resonance depends on the orbital eccentricity and the principal moments of inertia through $(B - A)/C$. As long as $(B - A)/C \ll 1$, averaging is a good approximation and the resulting spin states are orderly. However, the figure of Hyperion has been determined from Voyager 2 images (Smith *et al.*, 1982; T. C. Duxbury, 1983, personal communication) and $(B - A)/C \approx 0.26$. This is significantly larger than the hydrostatic value assumed in Peale (1978), and averaging is no longer an appropriate approximation. In fact, the resonance overlap criterion (Chirikov, 1979) predicts the presence of a large zone of chaotic rotation.

In this paper, we reexamine the problem of spin–orbit coupling for those cases where averaging is not applicable, with special emphasis on parameters appropriate for Hyperion. In the next section, the problem is recalled and the qualitative features of the nonlinear spin–orbit problem are discussed. One mechanism for the onset of chaos, the overlap of first-order resonances, is briefly reviewed and the resonance overlap criterion is used to predict the critical value of $(B - A)/C$ above which there is large-scale chaotic behavior. In Section III, the spin–orbit phase space is numerically explored using the surface of section method. The existence of the large chaotic zone is verified, and the critical value for the onset of chaos is compared to the prediction of the resonance overlap criterion. In Section II and III it is assumed that the spin axis is normal to the orbit plane. In Section IV the stability of this orientation is examined for the spin–orbit states, where it is shown that for principal moments appropriate for Hyperion the synchronous and 1/2 spin–orbit states are attitude unstable! In Section V rotation in the chaotic zone is also shown to be attitude unstable. The resulting three-dimensional tumbling motions are considered in Section VI, and shown to be fully chaotic. Consequences of these results for the tidal evolution of Hyperion are discussed in Section VII and it is concluded that Hyperion will probably be found to be chaotically tumbling. A summary follows in Section VIII.

II. SPIN–ORBIT COUPLING REVISITED

Consider a satellite whose spin axis is normal to its orbit plane. The satellite is assumed to be a triaxial ellipsoid with principal moments of inertia $A < B < C$, and C is the moment about the spin axis. The orbit is assumed to be a fixed ellipse with semimajor axis a, eccentricity e, true anomaly f, instantaneous radius r, and longitude of periapse $\tilde{\omega}$, which is taken as the origin of longitudes. The orientation of the satellite's long axis is specified by ϑ and thus $\vartheta - f$ measures the orientation of the satellite's long axis relative to the planet–satellite center line. This notation is the same as that of Goldreich and Peale (1966). Without external tidal torques, the equation of motion for ϑ (Danby, 1962; Goldreich and Peale, 1966) is

$$\frac{d^2\vartheta}{dt^2} + \frac{\omega_0^2}{2r^3} \sin 2(\vartheta - f) = 0, \qquad (1)$$

where $\omega_0^2 = 3(B - A)/C$ and units have been chosen so that the orbital period of the satellite is 2π and its semimajor axis is one. Thus the dimensionless time t is equal to the mean longitude. Since the functions r and f are 2π periodic in the time, the second term in Eq. (1) may be expanded in a Fourier-like Poisson series giving

$$\frac{d^2\vartheta}{dt^2} + \frac{\omega_0^2}{2} \sum_{m=-\infty}^{\infty} H\left(\frac{m}{2}, e\right) \sin(2\vartheta - mt) = 0.$$

The coefficients $H(m/2,e)$ are proportional to $e^{2|(m/2)-1|}$ and are tabulated by Cayley (1859) and Goldreich and Peale (1966). When e is small, $H(m/2,e) \approx -\frac{1}{2}e, 1, \frac{7}{2}e$ for $m/2 = \frac{1}{2}, 1, \frac{3}{2}$, respectively. The half-integer $m/2$ will be denoted by the symbol p.

Resonances occur whenever one of the arguments of the sine functions is nearly stationary, i.e., whenever $|(d\vartheta/dt) - p| \ll \frac{1}{2}$. In such cases it is often useful to rewrite the equation of motion in terms of the slowly varying resonance variable $\gamma_p = \vartheta - pt$,

$$\frac{d^2\gamma_p}{dt^2} + \frac{\omega_0^2}{2} H(p,e) \sin 2\gamma_p + \frac{\omega_0^2}{2} \sum_{n\neq 0} H\left(p + \frac{n}{2}, e\right) \sin(2\gamma_p - nt) = 0. \quad (2)$$

If ω_0 is small enough the terms in the sum will oscillate rapidly compared to the much slower variation of γ_p determined by the first two terms and consequently will give little net contribution to the motion. As a first approximation for small ω_0, then, these high-frequency terms may be removed by holding γ_p fixed and averaging Eq. (2) over an orbital period. The resulting equation is

$$\frac{d^2\gamma_p}{dt^2} + \frac{\omega_0^2}{2} H(p,e) \sin 2\gamma_p = 0$$

and is equivalent to that for a pendulum. The first integral of this equation is

$$I_p = \frac{1}{2}\left(\frac{d\gamma_p}{dt}\right)^2 - \frac{\omega_0^2}{4} H(p,e) \cos 2\gamma_p;$$

γ_p librates for $I_p < I_p^S$ and circulates for $I_p > I_p^S$, where the separating value $I_p^S = (\omega_0^2/4)|H(p,e)|$. For $I_p < I_p^S$ and $H(p,e) > 0$, γ_p librates about zero; while for $I_p < I_p^S$ and $H(p,e) < 0$, γ_p librates about $\pi/2$. In both cases the frequency of small-amplitude oscillations is $\omega_0\sqrt{|H(p,e)|}$. For $I_p = I_p^S$, γ_p follows the infinite period separatrix which is asymptotic forward and backward in time to the unstable equilibrium. The half-width of the resonance is characterized by the maximum value of $d\gamma_p/dt$ on the separatrix. When γ_p librates $|d\gamma_p/dt|$ is always less than this value which is equal to $\omega_0\sqrt{|H(p,e)|}$.

Averaging is most useful for studying the motion near a resonance when the resonance half-widths are much smaller than their separation. In this case, most solutions of the actual equation of motion differ from those of the averaged equations by only small regular oscillations resulting from the nonresonant, high-frequency terms. An important exception occurs for motion near the infinite-period separatrix which is broadened by the high-frequency terms into a narrow chaotic band (Chirikov, 1979). While the band is present for all values of ω_0 it is extremely narrow for small ω_0. Chirikov has given an estimate of the half-width of this chaotic separatrix, which is expressed in terms of the chaotic variations of the integral I_p, viz.,

$$w_p = \frac{I_p - I_p^S}{I_p^S} = 4\pi\varepsilon\lambda^3 e^{(-\pi\lambda)/2},$$

where ε is the ratio of the coefficient of the nearest perturbing high-frequency term to the coefficient of the perturbed term, and $\lambda = \Omega/\omega$ is the ratio of the frequency difference between the resonant term and the nearest nonresonant term (Ω) to the frequency of small-amplitude librations (ω). For the synchronous spin–orbit state perturbed by the $p = \frac{3}{2}$ term, $\varepsilon = H(\frac{3}{2},e)/H(1,e) = (7e)/2$ and $\lambda = 1/\omega_0$. Thus

$$w_1 = \frac{I_1 - I_1^S}{I_1^S} = \frac{14\pi e}{\omega_0^3} e^{-(\pi/2\omega_0)}. \quad (3)$$

For Mercury, for instance, where $\omega_0 = 0.017$ (for $(B - A)/C = 10^{-4}$) and $e = 0.206$, the width of the chaotic region associated with the synchronous state is $w_1 = 1.4 \times 10^{-34}$, and a similar estimate for the width of the $p = 3/2$ chaotic band gives $w_{3/2} = 5.4 \times 10^{-43}$! Averaging is certainly a good approximation for Mercury. On the other hand, the width of the chaotic layer depends exponentially on ω_0, and as ω_0 increases the size of the chaotic separatrix increases dra-

matically. Now most of the natural satellites are expected, on the basis of hydrostatic equilibrium, to have values of ω_0 larger than that expected for Mercury, in several cases approaching unity (Peale, 1977). At such large ω_0 chaotic separatrices are a major feature in the phase space. In studying the rotations of the natural satellites caution must be exercised when using the averaging method.

The widths of the libration regions also grow as ω_0 increases. At some point their widths, as calculated above using the averaging method, are so large that the resonances begin to overlap. Analyzed separately, libration would be expected in each of two neighboring resonances. However, simultaneous libration in two spin–orbit states is impossible. The result is widespread chaotic behavior. An estimate of the ω_0 at which this happens is provided by the Chirikov resonance overlap criterion. This criterion states that when the sum of two unperturbed half-widths equals the separation of resonance centers, large-scale chaos ensues. In the spin–orbit problem the two resonances with the largest widths are the $p = 1$ and $p = 3/2$ states. For these two states the resonance overlap criterion becomes

$$\omega_0^{RO}\sqrt{|H(1,e)|} + \omega_0^{RO}\sqrt{|H(3/2,e)|} = \frac{1}{2}$$

or

$$\omega_0^{RO} = \frac{1}{2 + \sqrt{14e}}. \qquad (4)$$

For $e = 0.1$, the mean eccentricity of Hyperion, the critical value of ω_0 above which large-scale chaotic behavior is expected is $\omega_0^{RO} = 0.31$. This is well below the actual value of Hyperion's ω_0 which has been determined from Voyager 2 images to be $\omega_0 = 0.89 \pm 0.22$ (T. C. Duxbury, 1983, personal communication). It is expected then that for Hyperion there is a large chaotic zone surrounding (at least) the $p = 1$ and $p = 3/2$ states, and possibly more.

These predictions are verified in the next section, where the spin–orbit phase space is investigated numerically using the surface of section method.

III. THE SPIN–ORBIT PHASE SPACE

Most Hamiltonian systems display both regular and irregular trajectories. The phase space is divided; there are regions in which trajectories behave chaotically and regions where trajectories are quasiperiodic (Hénon and Heiles, 1964). The simplest and most intuitive method of determining whether a trajectory is chaotic or quasiperiodic is the surface of section method. The spin–orbit problem, as defined in the last section, is 2π periodic in the dimensionless time. A surface of section is obtained by looking at the system stroboscopically with period 2π. A natural choice for the section is to plot $d\vartheta/dt$ versus ϑ at every periapse passage. The successive points define smooth curves for quasiperiodic trajectories; for chaotic trajectories the points appear to fill an area on the section in an apparently random manner. It is a remarkable property of Hamiltonian systems that these two types of behavior are usually readily distinguishable and that they are generally both present on any surface of section.

Because of the symmetry of a triaxial ellipsoid, the orientation denoted by ϑ is equivalent to that denoted by $\vartheta + \pi$. Consequently, ϑ may be restricted to the interval from 0 to π. The spin–orbit states found in the previous section by the averaging method are states where a resonance variable $\gamma_p = \vartheta - pt$ librates. For each of these states $d\vartheta/dt$ has an average value precisely equal to p, and ϑ rotates through all values. If attention is restricted, however, to the times of periapse passage, i.e., $t = 2\pi n$, then each γ_p taken modulo π is simply ϑ. A libration in γ_p becomes a libration in ϑ on the surface of section. For quasiperiodic libration successive points trace a simple curve on the section near $d\vartheta/dt = p$ which covers only a fraction of the possible interval from 0 to π. For nonresonant quasipe-

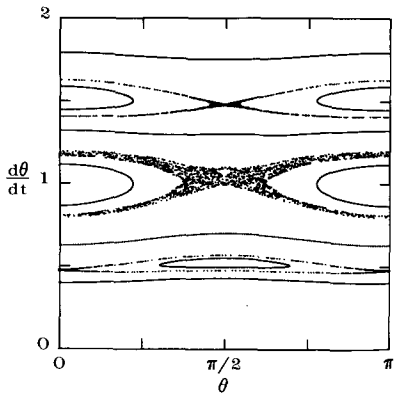

FIG. 1. Surface of section for $\omega_0 = 0.2$ and $e = 0.1$. $d\vartheta/dt$ versus ϑ at successive periapse passages for ten separate trajectories: three illustrating quasiperiodic libration, three illustrating the surrounding chaotic layers and four illustrating that quasiperiodic rotation separates the chaotic zones.

riodic trajectories, all γ_p rotate, and successive points on the surface of section will trace a simple curve which covers all values of ϑ. For small ω_0, resonant states are separated from nonresonant states by a narrow chaotic zone, for which successive points fill a very narrow area on the surface of section. The surface of section displayed in Fig. 1 illustrates these various possibilities for $\omega_0 = 0.2$ and $e = 0.1$. Equation (1) was numerically integrated for ten separate trajectories and $d\vartheta/dt$ was plotted versus ϑ at every periapse passage. Three trajectories illustrate quasiperiodic libration in the $p = 1$ (synchronous), $p = 1/2$, and $p = 3/2$ states. Three trajectories illustrate the chaotic separatrices surrounding each of these resonant states, and four trajectories show that each of these chaotic zones is separated from the others by impenetrable nonresonant quasiperiodic rotation trajectories. Five hundred successive points are plotted for each quasiperiodic trajectory, and 1000 points for each chaotic trajectory.

As ω_0 is increased both the resonance widths and the widths of the chaotic separatrices grow. The resonance overlap criterion predicts that the chaotic zones will begin to merge when $\omega_0 > \omega_0^{RO}$, where ω_0^{RO} is given by Eq. (1). For Hyperion, $e = 0.1$, and $\omega_0^{RO} = 0.31$. Numerically, we find that the $p = 1$ and $p = 3/2$ chaotic zones merge between $\omega_0 = 0.25$ and $\omega_0 = 0.28$. The prediction of the resonance overlap criterion is in excellent agreement with the numerical results, especially considering that ω_0 varies over two orders of magnitude for the natural satellites.

As ω_0 is further increased the simplicity of the picture developed for small ω_0 disappears. The now large chaotic zone surrounds more and more resonances, and the sizes of the principal quasiperiodic islands decrease. Figure 2 illustrates the main features of the surface of section for $e = 0.1$ and $\omega_0 = 0.89$, values appropriate for Hyperion. The chaotic sea is very large, surrounding all states from $p = 1/2$ to $p = 2$. Notice the change in scale from Fig. 1. The tiny remnant of the $p = 1/2$ island is in the lower center of the chaotic sea; the $p = 3/2$ island has disappeared altogether. The second-order $p = 9/4$ island in the top center of the chaotic zone is now one of the major features of the section. A total of 17 trajectories of Eq. (1) were used to generate this figure: eight quasiperiodic librators, illustrating the $p = 1/2$, 1, 2, 9/4, 5/2, 3, and 7/2 states, five nonresonant quasiperiodic rotators, and four chaotic trajectories (one for

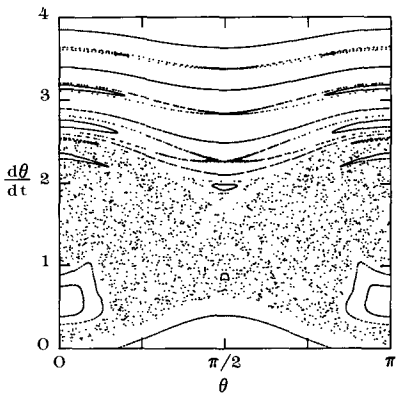

FIG. 2. Surface of section for $\omega_0 = 0.89$ and $e = 0.1$. Hyperion's spin–orbit phase space is dominated by a chaotic zone which is so large that even the $p = 1/2$ and $p = 2$ states are surrounded by it.

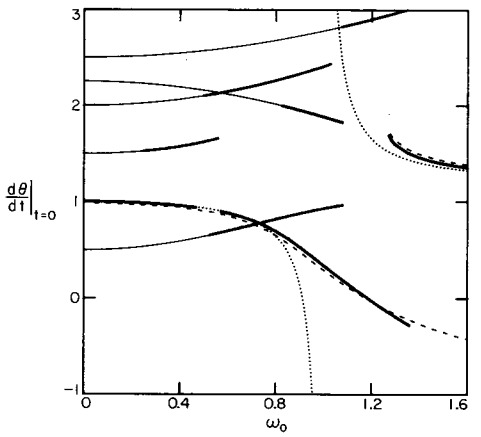

FIG. 3. Major island centers versus ω_0. Each island may be identified by the value of $d\vartheta/dt$ at $\omega_0 = 0$, except for the second synchronous branch which appears in the upper right quadrant. A broad line indicates that the island is surrounded by the large chaotic zone. These resonance curves summarize the surfaces of section by showing which states may be reached by traveling in the chaotic sea for any particular ω_0. The dotted lines show the usual linear approximation for the forced librations in the synchronous state, while the dashed lines show a much superior nonlinear approximation.

each chaotic zone). Two thousand points are plotted in the large chaotic sea.

While the average value of $d\vartheta/dt$ is precisely p for a quasiperiodic librator in state p, on the surface of section the island centers are displaced from these values. This displacement results from a forced libration with the same period as the orbital period and amplitude (in the variations of ϑ and $d\theta/dt$) equal to the displacement. This phenomenon is familiar from the forced libration of Phobos (Duxbury, 1977; Peale, 1977). A convenient way to summarize the results of the surfaces of section for various ω_0 is to plot the location of all the major island centers. The resonance centers occur at $\vartheta = 0$ or $\vartheta = \pi/2$, so it is sufficient to plot only $d\vartheta/dt$ versus ω_0. This plot is presented in Fig. 3 for an orbital eccentricity of 0.1. Curves with different symmetry may cross. For example, the $p = 1$ and $p = 1/2$ curves cross, yet the islands are always distinct since their centers occur at different values of ϑ. Whenever the island was surrounded by the large chaotic sea, the line has been broadened. The resonance curves in Fig. 3 thus give a clear picture of which states may be visited by traveling in the chaotic sea for any particular ω_0. It is interesting to note that for ω_0 within the range $1.27 < \omega_0 < 1.36$ two different synchronous islands are simultaneously present.

For the large ω_0 and e appropriate for Hyperion the forced librations are not well approximated by the linear theory that was used for Phobos. However, good approximations are obtained from the nonlinear method of Bogoliubov and Mitropolsky (1961). If we define $\psi_p = \vartheta - pf$ and Eq. (1) is rewritten with the true anomaly as the independent variable, the equation of motion for ψ_p becomes

$$(1 + e\cos f)\frac{d^2\psi_p}{df^2} - 2e\sin f\left(p + \frac{d\psi_p}{df}\right) + \frac{\omega_0^2}{2}\sin 2(\psi_p + (p-1)f) = 0. \quad (5)$$

The island centers are fixed points on the surface of section, thus $\psi_p(f)$ is 2π periodic. This suggests that ψ_p be written as a Fourier series, $\psi_p(f) = \psi_p{}^0 + \sum_{k=1}^{\infty} \psi_p{}^k \sin kf$. $\psi_p{}^0$ assumes a value of 0 or $\pi/2$ depending on whether libration is about ϑ equal to 0 or $\pi/2$, respectively, and only sine terms are included since the equation of motion is invariant under a simultaneous change in sign of ψ_p and f. A first approximation to the solution is obtained by retaining only the first term ($k = 1$) in this Fourier series. Substituting this into Eq. (5), multiplying by $\sin(f)$ and integrating from 0 to 2π yields an implicit equation for the amplitude $\psi_p{}^1$

$$\omega_0^2[J_{3-2p}(2\psi_p{}^1) + (-1)^{2p}J_{2p-1}(2\psi_p{}^1)] = (2\psi_p{}^1 + 4ep)(-1)^{(2\psi_p{}^0)/\pi}$$

where the J_i are the usual Bessel functions. The dashed line in Fig. 3 shows the solution to this equation for $p = 1$, where

$$\frac{d\vartheta}{dt} = \left(p + \frac{d\psi_p}{df}\right)\frac{df}{dt} = (p + \psi_p{}^1)\frac{(1+e)^2}{(1-e^2)^{3/2}}$$

on the surface of section (at periapse). Evidently, even one term in this Fourier series is a much better representation of the full solution than the usual linear solution (see Peale, 1977) which is drawn as a dotted line in Fig. 3. Though they are not drawn in Fig. 3 the nonlinear approximations for $p = 1/2$ and $p = 3/2$ are also quite good.

Up to now it has been assumed that the spin axis is perpendicular to the orbit plane. However, Fig. 2 bears little resemblance to the picture of spin–orbit coupling developed for small ω_0. In the next section this question of attitude stability is reevaluated in this now strongly nonlinear regime.

IV. ATTITUDE STABILITY OF ROTATION AT THE ISLAND CENTERS

Consider now the fully three-dimensional motion of a triaxial ellipsoid in a fixed elliptical orbit, which is specified as before. Let a, b, and c denote a right-handed set of axes fixed in the satellite, formed by the principal axes of inertia with moments $A < B < C$, respectively. In this case Euler's equations are (Danby, 1962)

$$A\frac{d\omega_a}{dt} - \omega_b\omega_c(B - C) = -\frac{3}{r^3}\beta\gamma(B - C),$$

$$B\frac{d\omega_b}{dt} - \omega_c\omega_a(C - A) = -\frac{3}{r^3}\gamma\alpha(C - A), \tag{6}$$

$$C\frac{d\omega_c}{dt} - \omega_a\omega_b(A - B) = -\frac{3}{r^3}\alpha\beta(A - B),$$

where ω_a, ω_b, and ω_c are the rotational angular velocities about the three axes a, b, and c, respectively, and α, β, and γ are the direction cosines of the planet to satellite radius vector on the same three axes.

To solve these equations, a set of generalized coordinates to specify the orientation of the satellite must be chosen. The Euler angles (as specified in Goldstein, 1965) are not suitable for this purpose because the resulting equations have a coordinate singularity when the spin axis is normal to the orbit plane, which is just the situation under study. A more convenient set of angles has therefore been chosen and is specified relative to an inertial coordinate system xyz which is defined at periapse. The x axis is chosen to be parallel to the planet to satellite radius vector, the y axis parallel to the orbital velocity, and the z axis normal to the orbit plane so as to complete a right-handed coordinate system. Three successive rotations are performed to bring the abc axes to their actual orientation from an orientation coincident with the xyz set of axes. First, the abc axes are rotated about the c axis by an angle ϑ. This is followed by a rotation about the a axis by an angle φ. The third rotation is about the b axis by an angle ψ. The first two rotations are the same as the Euler rotations, but their names have been interchanged. In terms of these angles the three angular velocities are

$$\omega_a = -\frac{d\vartheta}{dt}\cos\varphi\sin\psi + \frac{d\varphi}{dt}\cos\psi,$$

$$\omega_b = \frac{d\vartheta}{dt}\sin\varphi + \frac{d\psi}{dt},$$

$$\omega_c = \frac{d\vartheta}{dt}\cos\varphi\cos\psi + \frac{d\varphi}{dt}\sin\psi,$$

and the three direction cosines are

$$\alpha = \cos\psi\cos(\vartheta - f) - \sin\psi\sin\varphi\sin(\vartheta - f),$$

$$\beta = -\cos\varphi\sin(\vartheta - f),$$

$$\gamma = \sin\psi\cos(\vartheta - f) + \cos\psi\sin\varphi\sin(\vartheta - f).$$

The equations of motion for ϑ, φ, and ψ are then derived in a straightforward manner. For reference, the three canonically conjugate momenta are

$$p_\vartheta = -A\omega_a\cos\varphi\sin\psi + B\omega_b\sin\varphi + C\omega_c\cos\varphi\cos\psi,$$

$$p_\varphi = A\omega_a\cos\psi + C\omega_c\sin\psi,$$

$$p_\psi = B\omega_b.$$

When φ, ψ, p_φ and p_ψ are set equal to zero, they remain equal to zero. In this

equilibrium situation the spin axis is normal to the orbit plane and ϑ is identical to the ϑ used in the two previous sections. At the island centers $\vartheta(t)$ is periodic and the stability of this configuration may be determined by the method of Floquet multipliers (see, e.g., Poincaré, 1892; Cesari, 1963; Kane, 1965). A trajectory near this periodic trajectory is specified by $\vartheta' = \vartheta + \delta\vartheta$, $\varphi' = \varphi + \delta\varphi$, $\psi' = \psi + \delta\psi$, $p'_\vartheta = p_\vartheta + \delta p_\vartheta$, $p'_\varphi = p_\varphi + \delta p_\varphi$ and $p'_\psi = p_\psi + \delta p_\psi$. The equations of motion for the variations $\delta\vartheta$, $\delta\varphi$, $\delta\psi$, etc. are then linearized in the variations, giving six first-order linear differential equations with periodic coefficients. Integration of these equations over one period for six linearly independent initial variations ($\delta\vartheta = 1$, $\delta\varphi = \delta\psi = \delta p_\vartheta = \delta p_\varphi = \delta p_\psi = 0$; $\delta\vartheta = 0$, $\delta\varphi = 1$, $\delta\psi = \delta p_\vartheta = \delta p_\varphi = \delta p_\psi = 0$; etc.) defines a linear transformation which maps an arbitrary set of initial variations to their values one period later. The evolution of the variations over several periods is obtained by repeated application of this linear transformation. The eigenvalues of this linear transformation are called the Floquet multipliers, and determine the stability of the original periodic solution. Namely, if any of the Floquet multipliers have a modulus greater than one, then repeated application of the linear transformation will lead to exponential growth of the variations and the periodic solution is unstable; while (linear) stability is indicated if all the multipliers have modulus equal to one. Because of the Hamiltonian nature of this problem, every multiplier may be associated with another multiplier for which the product of the two moduli is equal to one (Poincaré, 1892). Thus instability is indicated by any multiplier with modulus not equal to one.

Two simplifications of this procedure were employed. Rather than explicitly linearize the equations of motion about the periodic reference trajectory, the variations were determined by directly integrating a nearby trajectory. The initial phase-space separation was taken to be 10^{-7}; the results are insensitive to this initial separation as long as it is small enough. The characteristic equation is a sixth-order polynomial equation, which is cumbersome to solve. Fortunately, it may be explicitly factored into the product of a quadratic equation, which determines the stability of the ϑ motion with the spin axis normal to the orbit plane, and a quartic equation which determines the attitude stability. Of course, the ϑ motion is always stable for the island centers.

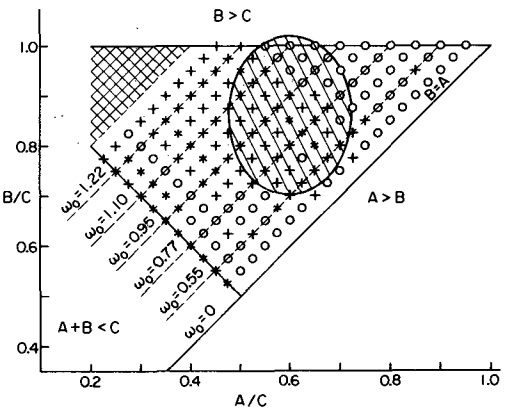

FIG. 4. Attitude stability diagram for the synchronous island center. A circle indicates stability, a plus sign indicates instability with one unstable direction and an asterisk indicates instability with two unstable directions. For most principal moments within the error ellipsoid of Hyperion the synchronous island is attitude unstable!

Figure 4 displays the results of a number of calculations of the Floquet multipliers for the centers of the synchronous islands, with $e = 0.1$, for various principal moments. Because Eqs. (6) are linear in the moments, it is sufficient to specify only the two principal moment ratios, A/C and B/C. A grid of these ratios was studied, with a basic grid step of 0.025 for both ratios. The dashed lines are lines of constant ω_0. Since the lower synchronous island disappears for $\omega_0 > 1.36$, this region has been hatched. Also, for ω_0 near 0.5, the synchronous island bifurcates into a period doubled pair of islands, neither of which is centered at $\vartheta = 0$. Consequently, for $\omega_0 = 0.55$ it was the

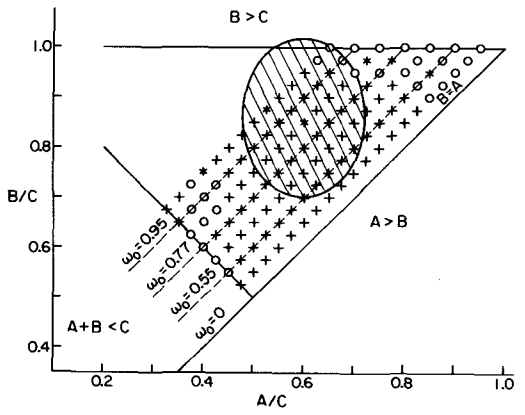

FIG. 5. Attitude stability diagram for the $p = 1/2$ island center. For principal moments within the error ellipsoid of Hyperion the $p = 1/2$ island is also mainly attitude unstable. The symbols are the same as those in Fig. 4.

attitude stability of this island pair which was studied. Whenever the Floquet analysis indicated stability a small circle is plotted. Instability is denoted by a plus sign if one pair of multipliers had moduli not equal to one, and by an asterisk if two pairs of multipliers had moduli not equal to one. The resulting regions of stability and instability are complicated, and it is expected that even more structure would be found if the grid size were reduced (Kane, 1965). The error ellipsoid for the actual figure of Hyperion, as determined by Duxbury, is also shown. The surprising result is that for most values of the principal moments within this ellipsoid, rotation at the synchronous island center is attitude unstable! Figures 5 and 6 show the results of similar calculations for the $p = 1/2$ and $p = 2$ island centers, respectively. Again, for most values of ω_0 within the error ellipsoid, rotation at the $p = 1/2$ island center is attitude unstable. On the other hand, except for a few isolated points, the $p = 2$ state is attitude stable. These isolated points of instability are associated with narrow lines of internal resonance, where the fundamental frequencies of small-amplitude oscillations are commensurate either among themselves or with the orbital frequency. The diagram for the $p = 9/4$ state is similar to that for the $p = 2$ state, and mainly indicates stability. The $p = 3/2$ state is likewise mainly stable, but exists only for $\omega_0 < 0.56$.

To summarize, for principal moments within the error ellipsoid for Hyperion the synchronous ($p = 1$) and $p = 1/2$ states are mainly attitude unstable, while the $p = 2$ and $p = 9/4$ states are stable. Except for certain moments of inertia near the edge of the error ellipsoid in Fig. 4, Hyperion has no stable synchronous state.

The method of Floquet multipliers is not suitable to determine the attitude stability of rotation in the chaotic zones since the reference trajectory is no longer periodic. For this purpose the Lyapunov characteristic exponents are introduced in the next section.

V. ATTITUDE STABILITY OF ROTATION IN THE CHAOTIC ZONE

The repeated application of a linear operator leads to exponential growth if one or more of its eigenvalues has modulus greater than one, and to oscillatory behavior if all the eigenvalues have moduli equal to one. The Floquet multipliers introduced in the last section are thus indicators of exponential deviation from the periodic trajectory.

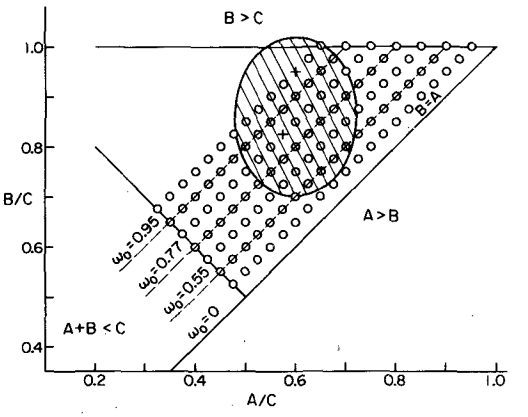

FIG. 6. Attitude stability diagram for the $p = 2$ island center. This state is predominantly attitude stable. The symbols are the same as those in Fig. 4.

They may be calculated from a characteristic equation determined from a numerical integration over one orbit period because the reference trajectory is periodic and the variations are being subjected to the same "forces" over and over again. When there is no underlying periodicity, the Floquet method is not useful. Rather, a measure of exponential separation is provided by the Lyapunov characteristic exponents (LCEs). The Lyapunov characteristic exponents play a dual role in this paper. In this section, they are defined and used to determine the attitude stability of the large chaotic zone, while in the next section they are used as indicators of chaotic behavior. (See Wisdom (1983) for more discussion of these exponents.)

The LCEs measure the average rate of exponential separation of trajectories near some reference trajectory. They are defined as

$$\lambda = \lim_{t\to\infty} \gamma(t) = \lim_{t\to\infty} \frac{\ln[d(t)/d(t_0)]}{t - t_0}, \quad (7)$$

where

$$d(t) = \sqrt{\delta\vartheta^2 + \delta\varphi^2 + \delta\psi^2 + \delta p_\vartheta{}^2 + \delta p_\varphi{}^2 + \delta p_\psi{}^2},$$

the usual Euclidean distance between the reference trajectory and some neighboring trajectory. The variations $\delta\vartheta$, $\delta\varphi$, $\delta\psi$, etc. satisfy the same six linear first-order differential equations as in the last section. The difference is that now the reference trajectory need no longer be periodic. In general, as the direction of the initial displacement vector is varied, λ may take at most N values, where N is the dimension of the system. In Hamiltonian systems, the λ_i are additionally constrained to come in pairs: for every $\lambda_i > 0$ there is a $\lambda_j < 0$, such that $\lambda_i + \lambda_j = 0$. Thus in the spin–orbit problem only three LCEs are independent; it is sufficient to only study those which are positive or zero. (For a review of the mathematical results regarding LCEs see Benettin *et al.* (1980a)).

In this section we are concerned with attitude stability. In all cases the reference trajectory has its spin axis normal to the orbit plane. An attitude instability is indicated if the spin axes of neighboring trajectories exponentially separate from the equilibrium orientation. If the reference trajectory is quasiperiodic then one pair of LCEs must be zero, and instability is indicated if any other LCE is nonzero. On the other hand, if the reference trajectory is chaotic, one LCE must be positive (see Section VI), and attitude instability is indicated if two or more LCEs are positive. In cases where the reference trajectory is periodic there is a correspondence between the Floquet multipliers, α_i, and the LCEs, λ_j, viz., for every i there is a j such that $\lambda_j = (\ln|\alpha_i|)/T$, where T is the period of the reference trajectory. For every Floquet multiplier with modulus greater than one, there is a Lyapunov exponent greater than zero.

The calculation of the largest LCE is not difficult, but to determine the attitude stability of the large chaotic zone it is necessary to determine at least the two largest LCEs, as one exponent must be positive to reflect the fact that the reference trajectory is chaotic. Because several different rates of exponential growth are simultaneously present, the numerical determination of more than the largest LCE is not a trivial task. The algorithm used here is that devised by Benettin *et al.* (1980b).

The infinite limit in Eq. (7) is of course not reached in actual calculations. If $\lambda = 0$, then $d(t)$ oscillates or grows linearly and $\gamma(t)$ approaches zero as $\ln(t)/t$. If, however, $\lambda \neq 0$ then $\gamma(t)$ approaches this nonzero limit. These two cases are easily distinguished on a plot of log $\gamma(t)$ versus log t, where the $\ln(t)/t$ behavior appears roughly as a line with slope -1. This is illustrated in Fig. 7 where calculations are presented of the three largest LCEs for the synchronous island center with moments appropriate for Hyperion ($A/C = 0.5956$ and $B/C = 0.8595$). Two LCEs are approaching a (positive) nonzero limit and one has the behavior ex-

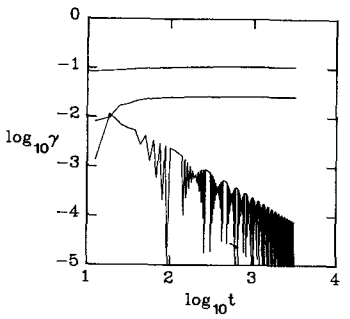

FIG. 7. Lyapunov characteristic exponents for the synchronous island center with moments appropriate for Hyperion. Two exponents are positive and the third has the behavior expected of a zero exponent.

pected of a zero exponent. This verifies the result of the Floquet analysis that with these moments rotation in the synchronous island is attitude unstable. As a further check, the attitude stability of all the synchronous island centers previously determined by the Floquet method were redetermined with the LCEs. In all cases the two methods agreed, both qualitatively and quantitatively.

Finally, the stability diagram for the large chaotic zone is shown in Fig. 8. For all values of A/C and B/C which were studied, reference trajectories in the large chaotic zone with axes perpendicular to the orbit plane have three positive LCEs. This indicates attitude instability; small displacements of the spin axis from the orbit normal grow exponentially for all trajectories in the large chaotic sea!

The LCEs also provide a time scale for the divergence of the spin axis from the orbit normal. Since neighboring trajectories separate from the reference trajectory as $e^{\lambda t}$, the e-folding time for exponential divergence is $1/\lambda$. For quasiperiodic (or periodic) reference trajectories the appropriate λ to use is the largest LCE; for chaotic reference trajectories the second-largest LCE is appropriate since at least one of the first two is associated with attitude instability. For values of the principal moments near those of Hyperion these λ's are both near 0.1. The e-folding time is thus of order 10 or only two orbital periods! These attitude instabilities are very strong.

VI. CHAOTIC TUMBLING

Almost all trajectories initially near a chaotic reference trajectory separate from it exponentially on the average, while almost all trajectories initially near a quasiperiodic reference trajectory separate from it roughly linearly. Chaotic behavior can thus be detected by examining the behavior of neighboring trajectories. The rate of exponential divergence of nearby trajectories is quantified by the Lyapunov characteristic exponents which were introduced in the last section. A nonzero LCE indicates that the reference trajectory is chaotic. If all of the LCEs are zero then the reference trajectory is quasiperiodic. More generally, every pair of zero exponents indicates the existence of an "integral" of the motion. The trajectory is "integrable" if all LCEs are zero.

In the previous two sections several cases of attitude instability were found. However, the methods used are only indicators of linear instability since the equations of motion for the variations were linearized. It is possible that when the orientation of the spin axis normal to the

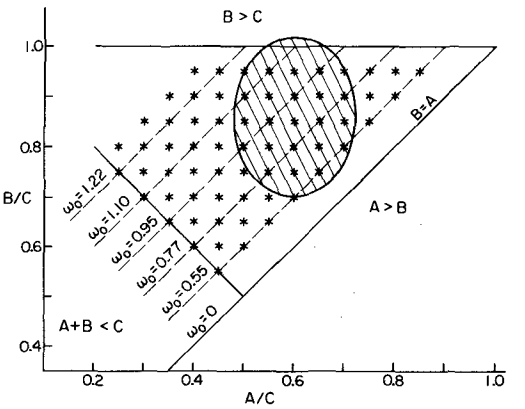

FIG. 8. Attitude stability diagram for the large chaotic zone. In all cases studied the large chaotic zone is attitude unstable.

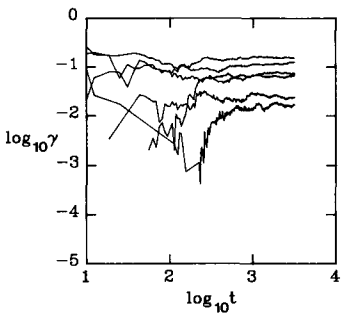

FIG. 9. Three Lyapunov characteristic exponents for two trajectories whose axes were initially slightly displaced from the orbit normal. The resulting tumbling motion is fully chaotic; there are no zero exponents. The LCEs for the two trajectories are approaching similar values.

orbit plane is unstable, the spin axis nevertheless remains near that orientation or periodically returns to it. This turns out not to be the case. Wherever the linear analyses indicated instability a trajectory slightly displaced from the equilibrium orientation was numerically integrated. In every case, the spin axis subsequently went through large variations and the c body axis went more than 90° from its original orientation perpendicular to the orbit plane. Still, these large excursions could be of a periodic or quasiperiodic nature.

A calculation of the LCEs for one of these trajectories which originates near the equilibrium has been made to answer this question. The algorithm of Benettin *et al.* (1980b) was again used to avoid the numerical difficulties in calculating several LCEs. However, an additional difficulty was encountered, namely, the equations of motion as described in Section IV become singular when $\varphi = \pi/2$. At this point the θ rotation and the ψ rotation become parallel. Since all of the angles go through large variations this singularity is frequently encountered. To navigate past this coordinate singularity, a change of coordinates was made to the usual Euler angles, which are singular at $\varphi_E = 0$. (The first two Euler rotations are the same as those used here, but the third is a rotation about the c axis by the angle ψ_E. When $\varphi_E = 0$, the ϑ_E and the ψ_E rotations are parallel.) Figure 9 shows the results for two trajectories with initial conditions $\varphi = 0.1$, $\psi = 0.01$, $d\varphi/dt = 0$, $d\psi/dt = 0$, and $d\vartheta/dt = 1$. One of them began with $\vartheta = \pi/2$ and the other at $\vartheta = \pi/2 + 1/2$. The principal moments are $A/C = 0.5956$ and $B/C = 0.8595$, values appropriate for Hyperion. The initial conditions are such that the ϑ motion by itself would be chaotic, i.e., the trajectory with the axis of rotation fixed perpendicular to the orbit plane would lie in the large chaotic zone. The three LCEs for the two trajectories are approaching roughly the same limits. The results show clearly that the tumbling motion is fully chaotic; none of the LCEs is zero.

VII. TIDAL EVOLUTION

We have seen many qualitatively new features in the rotational behavior of satellites with large ω_0 in eccentric orbits. New features also appear in their tidal evolution. In general, tidal dissipation tends to drive the spin rate of a satellite to a value near synchronous (e.g., Peale and Gold, 1965). In this process the satellite has most likely passed through several stable spin–orbit states where libration of its spin angular velocity about a nonsynchronous value could be stabilized against further tidal evolution by the gravitational torque on the permanent asymmetry of the satellite's mass distribution. Whether or not the satellite will be captured as it encounters one of these spin–orbit states depends on the spin angular velocity as the resonance variable γ_p enters its first libration. If the spin rate is below a critical value capture results, and otherwise the satellite passes through the resonance. In most situations there is not enough information to determine if this condition is satisfied and capture probabilities may be calculated by introducing a suitable probability distribution over the initial angular velocity. For instance, the capture probability may be defined as the ratio of range of the first integral I_p which leads to

capture to the total range of I_p allowing a first libration (Goldreich and Peale, 1966).

This standard picture of the capture process implicitly assumes that the behavior near the separatrix is regular and thus well described by the averaged equations of motion. In general, though, the motion near a separatrix in a nonlinear dynamical system is not regular but chaotic. The calculation of capture probabilities is a well-developed art (see Henrard, 1982; Borderies and Goldreich, 1984), but the effect of the chaotic separatrix has never been mentioned. Of course, when ω_0 is very small the chaotic separatrix is microscopically small, and even a very small tidal torque can sweep the system across the chaotic zone so quickly that it has essentially no effect. On the other hand, for larger ω_0 where the chaotic zones are sizable, the simple capture process described above is qualitatively incorrect. While still fundamentally deterministic, the capture process now involves the randomness inherent in deterministic chaos. Probabilities still arise from unknown initial conditions, but now the outcome is an extremely sensitive, essentially unpredictable function of these initial conditions. The capture process is more properly viewed as a random process.

Following Goldreich and Peale (1966), let ΔE denote the change in the integral I_p over one cycle of the resonance variable γ_p due to the tidal torque. When ΔE is much smaller than the width of the chaotic separatrix $2w_pI_p$ the chaotic character of the separatrix may be expected to have a significant effect on the capture process. For the $p = 3/2$ state of a nearly spherical body this condition is

$$\frac{15k_2R^3}{8\,\mu Q} < \left(\frac{2}{7e}\right)^{3/2} \frac{1}{\omega_0}\, e^{-\pi/(\omega_0\sqrt{14e})},$$

where k_2 is the Love number, $1/Q$ is the specific dissipation function, R is the ratio of the radius of the body to the orbit semimajor axis, and μ is the satellite to planet mass ratio. With parameters appropriate for Mercury this inequality is satisfied for all $\omega_0 > 0.075$. This critical ω_0 is only a little more than four times Mercury's actual ω_0 as assumed in Goldreich and Peale (1966)! The chaotic separatrix should not be blithely ignored.

If ω_0 is much larger a trajectory may spend a considerable amount of time in a chaotic zone before escaping or being captured. Motion in a chaotic zone depends extremely sensitively on the initial conditions. Capture will occur if, by chance, the trajectory spends enough time near the border of the libration zone for the tidal dissipation to take it out of the chaotic region; escape occurs if, by chance, the trajectory spends enough time near the border of regular circulation for the tidal dissipation to move it into the regular region. For a value of ω_0 as large as that of Hyperion, the picture is even more complicated since many islands are accessible to a traveler in the large chaotic sea. Once a trajectory has entered the large chaotic zone, it may repeatedly visit each of the accessible states before finally being captured by one of them. In numerical experiments, this odyssey frequently takes a very long time, as compared to capture without a chaotic zone where capture or escape is decided permanently on a single pass through a resonance. These experiments were performed with principal moments appropriate for Hyperion, the spin axis normal to the orbit plane and a tidal torque given by

$$T = -\frac{C\, d(\vartheta - f)}{r^6\, dt}$$

which is appropriate when the tidal phase lag is simply proportional to the frequency (Goldreich and Peale, 1966). The constant C was chosen for computational convenience to be of order 10^{-3}. Capture in each accessible state appears to be possible, though the synchronous state was the most common endpoint.

Normally, tidal dissipation not only drives the spin rate toward a value near

synchronous, but also drives the spin axis to an orientation normal to the orbit plane. Thus, in Goldreich and Peale (1966), for instance, this orientation for the spin axis is simply assumed. The discussion of tidal evolution is now complicated by the rather surprising results of Sections IV, V, and VI where it was found that in many cases the orientation of the spin axis perpendicular to the orbit plane is unstable. In particular, the large chaotic zone is attitude unstable (Section V). So as soon as the large chaotic zone is entered the spin axis leaves its preferred orientation and begins to tumble chaotically through all orientations (Section VI). Capture into one of the attitude-stable islands is still a possibility. However, for Hyperion, the only attitude-stable endpoints which are accessible, once the large chaotic sea has been entered, are the $p = 2$ and $p = 9/4$ states. The synchronous and $p = 1/2$ states are attitude unstable for most values of the principal moments within the error ellipsoid of Hyperion and the $p = 3/2$ state does not exist for ω_0 above 0.56 (Section IV). Occasionally, the tumbling satellite may come near one of the attitude-stable islands with its spin axis perpendicular to the orbit plane. If it lingers long enough it may be captured. However, the chaotic zone is strongly chaotic ($\lambda \approx 0.1$) and the tidal dissipation is very weak (the time scale for the despinning of Hyperion is of the order of the age of the Solar System). It may take a very long time for this tumbling satellite to enter an orientation favorable for capture to occur. Judging from the long times required in the numerical experiments for capture to occur even when the spin axis was fixed in the required direction it seems to us unlikely that Hyperion has been captured. We expect that Hyperion will be found to be tumbling chaotically.

Preliminary observations of a 13-day period (Thomas *et al.*, 1984; Goguen, 1983) support this conclusion that capture has not occurred. We should point out that the traditional method of determining periods from light variations involves observations which are separated by times longer than the period of variation and the period is determined by folding these observations back on each other with an assumed period which is varied until the scatter of points about a smooth curve is minimized. This method will not yield meaningful results if the period of the observed object varies markedly on a time scale which is short compared to the time spanning the observations. Hence the determination of a chaotic light curve requires many magnitude observations per orbit period carried out over several orbit periods.

VIII. SUMMARY

Hyperion's highly aspherical mass distribution and its large, forced orbital eccentricity renders inapplicable the usual theory of spin orbit coupling which relies on the averaging method. In fact, for much smaller $(B - A)/C$ the resonance overlap criterion predicts the presence of a large chaotic zone in the spin–orbit phase space, and numerical exploration using the surface of section method has verified its presence. For Hyperion, this chaotic zone is so large that it engulfs all states from the $p = 1/2$ state to the $p = 2$ state. The $p = 3/2$ state has disappeared altogether, and the second-order $p = 9/4$ island is a prominent feature on the surface of section.

Hyperion could stably librate in the synchronous spin–orbit state if the spin axis were able to remain normal to the orbit plane. However, for most values of the principal moments within the error ellipsoid for Hyperion, Floquet stability analysis indicates that rotation within the synchronous island is attitude unstable. A small initial displacement of the spin axis from the orbit normal grows exponentially and the axis appears to pass through all orientations. Likewise, the $p = 1/2$ state is attitude unstable for most principal moments near those estimated for Hyperion. The only attitude-stable islands in the large chaotic sea are the $p = 2$ and $p = 9/4$ states.

The orientation of the spin axis perpendicular to the orbit plane is likewise unstable for trajectories in the large chaotic zone. This is indicated by the Lyapunov characteristic exponents which measure the rate of exponential separation of neighboring trajectories. Small displacements of the spin axis from the orbit normal lead to large displacements. Lyapunov characteristic exponents for the resulting tumbling motion indicate that it is fully chaotic; there are no zero exponents.

Over the age of the solar system, tidal dissipation can drive Hyperion's spin to a near synchronous value. The probability of the spin being captured into any of the spin–orbit states with $p > 2$ is negligibly small, and Hyperion will have necessarily entered the large chaotic zone. At this point, Hyperion's spin axis becomes attitude unstable, and Hyperion begins to tumble chaotically with large, essentially random variations in spin rate and orientation. Tidal dissipation may lead to capture if Hyperion's spin comes close enough to one of the attitude-stable islands with its spin axis perpendicular to the orbit plane. However, judging from the long times required in numerical experiments for capture to occur even when the spin axis was fixed in the required orientation and the fact that the tidal dissipation is very weak (the time scale for the despinning of Hyperion is on the order of one billion years), it seems to us unlikely that capture has occurred. We expect that Hyperion will be found to be tumbling chaotically as more extensive observations conclusively define its rotation state. If this chaotic tumbling is confirmed, Hyperion will be the first example of chaotic behavior among the permanent members of the solar system.

ACKNOWLEDGMENTS

We gratefully acknowledge informative discussions with Dale Cruikshank, Mert Davies, Tom Duxbury, Jay Goguen, Michael Nauenburg, Peter Thomas, and Charles Yoder. Special thanks are due D. Cruikshank and T. Duxbury who kindly provided their observational data before publication and to Donald Hitzl who pointed out some important references. This work was supported in part by the NASA Geochemistry and Geophysics Program under Grant NGR 05 010 062.

REFERENCES

BENETTIN, G., L. GALGANI, A. GIORGILLI, AND J.-M. STRELCYN (1980a). Lyapunov characteristic exponents for smooth dynamical systems and for Hamiltonian systems; a method for computing all of them: Part 1. Theory. *Meccanica* March, 9–20.

BENETTIN, G., L. GALGANI, A. GIORGILLI, AND J.-M. STRELCYN (1980b). Lyapunov characteristic exponents for smooth dynamical systems and for Hamiltonian systems; a method for computing all of them: Part 2. Numerical application. *Meccanica* March, 21–30.

BORDERIES, N., AND P. GOLDREICH (1984). A simple derivation of capture probabilities for the J + 1 : J and J + 2 : J orbit–orbit resonance problems. Submitted for publication.

BOGOLIUBOV, N. N., AND Y. A. MITROPOLSKY (1961). *Asymptotic Methods in the Theory of Non-Linear Oscillations*. Hindustan, Delhi.

CAYLEY, A. (1859). Tables of the developments of functions in the theory of elliptic motion. *Mem. Roy. Astron. Soc.* **29,** 191–306.

CESARI, L. (1963). *Asymptotic Behavior and Stability Problems in Ordinary Differential Equations*. Springer-Verlag, Berlin/New York.

CHIRIKOV, B. V. (1979). A universal instability of many-dimensional oscillators systems. *Phys. Rep.* **52,** 263–379.

DANBY, J. M. A. (1962). *Fundamentals of Celestial Mechanics*. Macmillan, New York.

DUXBURY, T. C. (1977). Phobos and Deimos: Geodesy. In *Planetary Satellites* (J. Burns, Ed.), pp. 346–362. Univ. of Arizona Press, Tucson.

GOGUEN, J. (1983). Paper presented at IAU Colloquium 77, Natural Satellites, Ithaca, N.Y., July 5–9.

GOLDREICH, P., AND S. J. PEALE (1966). Spin–orbit coupling in the solar system. *Astron. J.* **71,** 425–438.

GOLDSTEIN, H. (1965). *Classical Mechanics*. Addison-Wesley, Reading.

HÉNON, M. AND C. HEILES (1964). The applicability of the third integral of motion: Some numerical experiments. *Astron. J.* **69,** 73–79.

HENRARD, J. (1982). Capture into resonance: an extension of the use of adiabatic invariants. *Celest. Mech.* **27,** 3–22.

KANE, T. R. (1965). Attitude stability of Earth-pointing satellites. *AIAA J* **3,** 726–731.

PEALE, S. J. (1977). Rotation histories of the natural satellites. In *Planetary Satellites* (J. Burns, Ed.), pp. 87–112. Univ. of Arizona Press, Tucson.

PEALE, S. J. (1978). An observational test for the origin of the Titan–Hyperion orbital resonance. *Icarus* **36,** 240–244.

PEALE, S. J., AND T. GOLD (1965). Rotation of the planet mercury. *Nature* **206,** 1240–1241.

POINCARÉ, H. (1892). *Les Méthodes Nouvelles de la Mécanique Céleste*. Gauthier-Villars, Paris.

SMITH, B., *et al.* (1982). A new look at the Saturn system: The Voyager 2 images. *Science* **215,** 504–537.

THOMAS, P., J. VEVERKA, D. WENKERT, E. DANIELSON, AND M. DAVIES (1984). Voyager photometry of Hyperion: Rotation rate. Paper presented at IAU Colloquium 77, Natural Satellites, Ithaca, N.Y., July 5–9. Submitted for publication.

WIDORN, T. (1950). Der lichtwechsel des Saturnsatelliten Japetus in jahre 1949. *Sitzungsber. Osterr. Akad. Wiss., Wiem, Abt IIa,* **159,** 189–199.

WISDOM, J. (1983). Chaotic behavior and the origin of the 3/1 Kirkwood gap. *Icarus* **56,** 51–74.